EFFECTS OF PHASE ANGLE AND SENSOR TEMPERATURE ON THE OBSERVED CONTINUUM-REMOVED M³ REFLECTANCE AND INFERRED SPECTRAL PARAMETERS. A. Grumpe[1], V. Zirin[1] and C. Wöhler[1] [1]Image Analysis Group, TU Dortmund University, D–44227 Dortmund, Germany; {arne.grumpe | vladimir.zirin | christian.woehler}@tu-dortmund.de

Introduction: The Moon Mineralogy Mapper (M^3) instrument carried by the Indian spacecraft Chandrayaan-1 provides lunar hyperspectral radiance data. The dataset of nearly global coverage was initially released in two parts (v1 and v2) at the Planetary Data System: http://m3.jpl.nasa.gov/m3data.html. For brevity, we refer to this release as v1 dataset. Recently a new release of the data (v3) provided additional compensation of the sensor temperature which had not been included in the previous release [1].

Within our previous work based on the v1 dataset, we found that after normalisation of the spectral data using the Hapke model [2] that the normalised reflectance measured at the same surface pixel changes with respect to the phase angle [3]. Furthermore, the parameters describing the spectral absorption bands, namely the position of the absorption minimum (λ_{abs}) and the relative depth of the absorption trough after continuum removal (δ_{abs}), are heavily distorted. We refer to these quantities as spectral parameters. The distortion is correlated with the phase angle [4].

In this study we present an empirical correction of the continuum-removed (CR) M³ reflectance spectra with respect to the phase angle.

Spectral normalisation: To analyse spectral data accurately, the measured reflectances have to be normalised to a common reference illumination and viewing geometry (incidence angle $\vartheta_i = 30°$, emission angle $\vartheta_e = 0°$ and phase angle $\alpha = 30°$ [5]), which is performed by estimating the pixel-wise single-scattering albedo of the Hapke model [2, 4] and, for comparison, by applying the empirical model proposed by Hicks et al. [6] to the v1 data. For the v3 data, the empirical normalisation coefficients had not been published yet while this study was carried out, such that solely the Hapke model was applied. A smoothing spline is adapted to the spectra, and the continuum is removed by division by the convex hull [7]. The subsequent analysis is based on the CR spectra to accentuate small spectral parameter variations.

Data selection: To measure the distortion of the CR spectra, we searched the dataset for regions with images acquired at a phase angle of $\alpha = 30° \pm 2°$. From these candidates, 25 regions of 2° by 2° size were selected to include samples from as many different regions as possible (cf. Fig. 1). However, for the four regions marked in red colour no images at different phase angles were available, and the regions were omitted. Additionally, mare regions were excluded since the amount of available data was not sufficient.

Empirical correction: The distortion of the CR spectra after normalisation with the Hapke model shows a phase angle dependence. Thus, we computed the corrected CR reflectance $\hat{R}$ from the Hapke-normalised CR reflectance R using

$$\hat{R} = a(\alpha)R + b(\alpha)$$

where $a(\alpha) = a_1 \Delta\alpha + a_0$, $b(\alpha) = b_1 \Delta\alpha + b_0$, and $\Delta\alpha = \alpha - 30°$ measures the deviation from the reference geometry. The coefficients a_0, a_1, b_0 and b_1 are

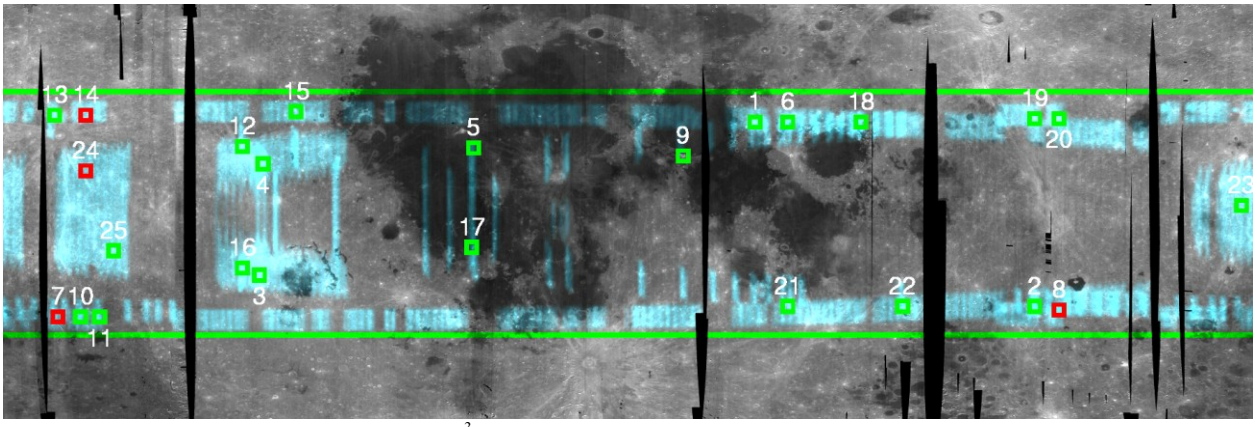

Fig. 1: Global photometrically normalised M^3 mosaic from 60° S to 60° N. The green line marks the 30° latitude boundary. The examined regions reside within this boundary. The selected regions are marked as rectangles. Red rectangles mark omitted regions that do not contain images at different phase angles. The bluish shade denotes the number of pixels illuminated at 30° ± 2° phase angle.

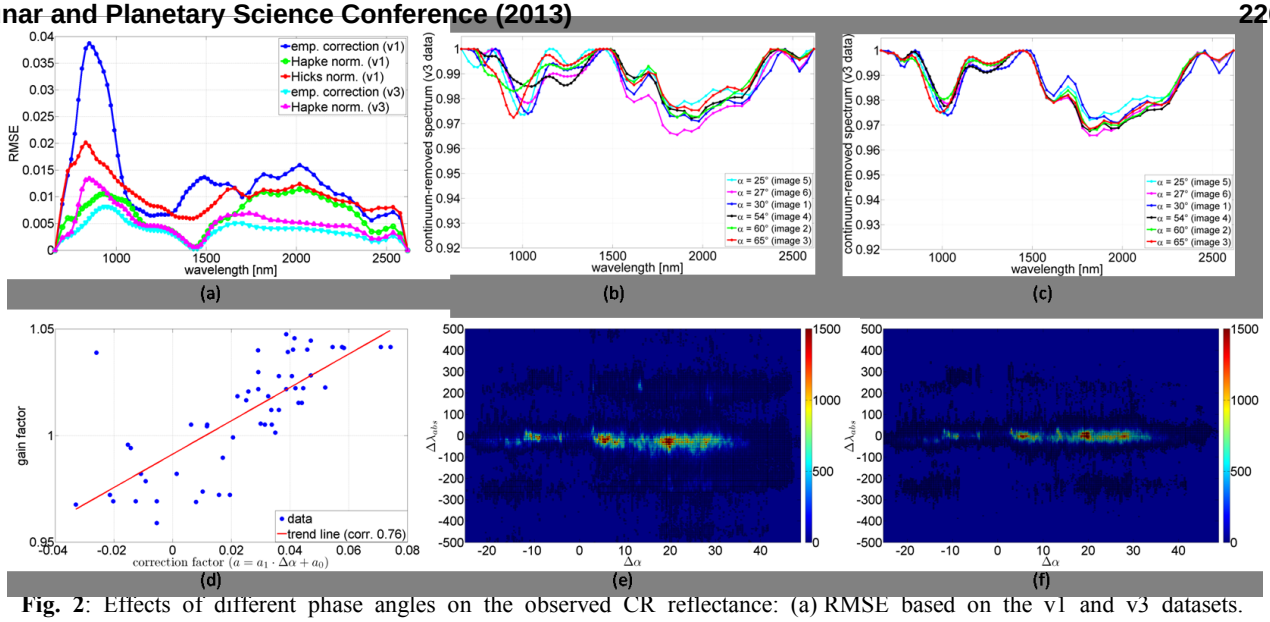

Fig. 2: Effects of different phase angles on the observed CR reflectance: (a) RMSE based on the v1 and v3 datasets. (b) Typical observed CR reflectance before correction (v3 dataset). (c) Typical observed CR reflectance after correction (v3 dataset). (d) Gain factors (sensor temperature) and empirical correction factors for M³ channel 17. (e) Absorption wavelength λ_{abs} before correction. (f) Absorption wavelength λ_{abs} after correction.

computed channel-wise using the selected regions by linear least squares regression. The CR reflectance acquired at the phase angle closest to 30° is chosen as the target CR reflectance. To avoid the influence of topography, only pixels with surface slopes of less than 2° inferred from a local DEM [4] are considered.

Results: Fig. 2 shows the results of the empirical correction. The root mean squared error (RMSE) is computed for the Hapke [2, 4] and Hicks [6] normalisation methods channel-wise over all pixels. In case of the empirical correction the leave-one-out model error estimation technique is applied, where for each region a set of parameters is estimated based on the remaining regions. The global error value is then derived from the individual errors.

The Hapke-normalised v1 dataset shows a strong distortion of the ferrous absorption trough near 1000 nm, which is less pronounced in the case of the Hicks normalisation method [6] (cf. Fig 2a). This normalisation estimates a gain factor as a polynomial in the phase angle and thus implicitly includes an empirical gain factor. However, the empirical method presented in this study focuses on the CR reflectance rather than the observed reflectance and thus yields a lower RMSE than the Hicks method [6].

The Hicks method [6] is not calibrated on the v3 data set and therefore has not been evaluated on that data set. The Hapke normalisation [2, 4] shows a strongly decreased RMSE on the v3 dataset. This might be due to the high correlation between the gain factor of the detector temperature [1] and the empirical phase angle dependent gain (cf. Fig. 2d) (correlation coefficient is 0.76). The empirical correction is still beneficial although it is not clear whether this effect is due to the phase angle or to imperfections of the sensor temperature calibration.

The CR reflectance of a typical observation before and after correction is displayed in Fig. 2b and c. Without empirical correction, a strong spread over all observations is observed, and the centre wavelength of the ferrous absorption trough shows a phase angle dependent shift. Our empirical correction strongly reduces these variations (Fig. 2e and f), especially in the case of large phase angles.

Summary and Conclusion: The empirical method presented in this study reveals a distortion of the observed CR spectra at different phase angles and the inferred spectral parameters. Possibly, these variations correspond to a photometric phase angle effect, but they may also be the result of imperfect detector temperature calibration, since we observed a strong correlation between the sensor temperature correction factors according to [1] and the observed distortions of the spectral parameters. Future work will include a comparison of our empirical method with the recently proposed v3 reflectance calibration [8].

References: [1] Lundeen, S. et. al. (2011) JPL D-39032, http://pds-imaging.jpl.nasa.gov/data/m3/CH1M3_0003/DOCUMENT/DPSIS.PDF [2] Hapke B. W. (2002) *Icarus 157*, 523–534; [3] Grumpe, A., Wöhler, C. (2011) *Proc. 7th IEEE Int. Symp. Image and Signal Proc. and Anal.*, 609-614; [4] Grumpe, A. et al. (2012) *Proc. European Lunar Symp.*, 34-35; [5] Pieters, C. M. (1999) *Proc. Workshop New Views of the Moon*, abstract #8025; [6] Hicks, M. D. et al. (2011) *J. Geophys. Res. 116*, E00G15; [7] Fu, Z. et al. (2007) *IEEE Trans. Geoscience and Remote Sensing 45(11)*, 3827-3844; [8] Besse, S. et al. (2013) *Icarus 222(1),* 229-242.